0026-895X/07/7103-930–941$20.00
MOLECULAR PHARMACOLOGY
Vol. 71, No. 3
30031/3182634
Mol Pharmacol 71:930–941, 2007
Printed in U.S.A.

Activation of the CXCR3 Chemokine Receptor through Anchoring of a Small Molecule Chelator Ligand between TM-III, -IV, and -VI[S]

Mette M. Rosenkilde, Michael B. Andersen, Rie Nygaard, Thomas M. Frimurer, and Thue W. Schwartz

Laboratory for Molecular Pharmacology, Department of Pharmacology, University of Copenhagen, Copenhagen, Denmark (M.M.R., M.B.A., R.N., T.W.S.); and 7TM Pharma A/S, Hørsholm, Denmark (R.N., T.M.F., T.W.S.)

Received August 21, 2006; accepted December 12, 2006

ABSTRACT

Seven transmembrane segment (7TM) receptors are activated through a common, still rather unclear molecular mechanism by a variety of chemical messengers ranging from monoamines to large proteins. By introducing a His residue at position III:05 in the CXCR3 receptor a metal ion site was built between the extracellular ends of transmembrane (TM) III and TM-IV to anchor aromatic chelators at a location corresponding to the presumed binding pocket for adrenergic receptor agonists. In this construct, free metal ions had no agonistic effect in accordance with the optimal geometry of the metal ion site in molecular models built over the inactive form of rhodopsin. In contrast, the aromatic chelators bipyridine or phenanthrolene in complex with Zn(II) or Cu(II) acted as potent agonists displaying signaling efficacies similar to or even better than the endogenous chemokine agonists. Molecular modeling and molecular simulations combined with mutational analysis indicated that the metal ion site-anchored chelators act as agonists by establishing an aromatic-aromatic, second-site interaction with TyrVI:16 on the inner face of TM-VI. It is noteworthy that this interaction required that the extracellular segment of TM-VI moves inward in the direction of TM-III, whereby TyrVI:16 together with the chelators complete an "aromatic zipper" also comprising PheIII:08 (corresponding to the monoamine receptor anchoring point) and TyrVII:10 (corresponding to the retinal attachment site in rhodopsin). Chemokine agonism was independent of this aromatic zipper. It is proposed that in rhodopsin-like 7TM receptors, small-molecule compounds in general act as agonists in a similar manner as here demonstrated with the artificial, metal ion site anchored chelators, by holding TM-VI bent inward.

Seven transmembrane segment (7TM) or G-protein-coupled receptors constitute the largest family of proteins in the human genome being activated by a very broad variety of chemical messengers and odor and taste components: from calcium ions to large glycoprotein hormones over all kinds of small molecules such as monoamines, amino acids, purines, lipids, and neuropeptides as well as larger peptide hormones and small proteins, such as chemokines (Bockaert and Pin, 1999; Lefkowitz, 2004).

Several X-ray structures have been generated for rhodopsin, but they all represent the same inactive, dark state of the molecule (Palczewski et al., 2000; Li et al., 2004; Okada et al., 2004). Even the structure of metarhodopsin-I, in which the inverse agonist 11-*cis*-retinal is converted to the all-*trans*, agonist form, has a very similar overall protein structure compared with the inactive state of the protein (Ruprecht et al., 2004). It is known from a number of biochemical and biophysical studies, however, that major conformational changes occur in the receptor protein during the subsequent transformation into the active, signaling metarhodopsin-II form (Sakmar et al., 2002; Hubbell et al., 2003). In particular, the comprehensive, site-directed spin labeling studies by Hubbell and Khorana and coworkers (Farrens et al., 1996; Hubbell et al., 2003) have shown that during activation, the intracellular segments of the transmembrane helices—especially TM-VI—undergo relatively large-amplitude, rigid-body movements

This study was supported by grants from the Novo Nordisk Foundation, the Danish Medical Research Council and from the European Community's Sixth Framework Program (grant LSHB-CT-2003-503337 and LSHB-CT-2005-518167).

Article, publication date, and citation information can be found at http://molpharm.aspetjournals.org.

doi:10.1124/mol.106.030031.

[S] The online version of this article (available at http://molpharm.aspetjournals.org) contains supplemental material.

ABBREVIATIONS: 7TM, seven transmembrane segment; NOE, nuclear Overhauser effect; TM, transmembrane segment; EPR, electron paramagnetic resonance; RMSD, root-mean-square deviation; IP3, inositol trisphosphate; CXCR3, chemokine CXC receptor type 3; IP10, chemokine CXC ligand 10; ITAC, chemokine CXC ligand 11.

away from each other and thereby reveal activating receptor epitopes for downstream signaling molecules. A number of biochemical and biophysical studies, especially in the β_2-adrenergic receptor support this picture (Gether et al., 1997; Ballesteros et al., 2001).

Only rather limited information is available concerning movements of the extracellular segments of the TMs. However, based on the distance constraints imposed by a number of activating metal ion sites constructed between TM-III, -VI, and -VII, we recently proposed a "global toggle switch" activation model for 7TM receptors (Elling et al., 2006). According to this model, an inward movement of the extracellular segments—especially TM-VI and TM-VII—was suggested to be coupled to the well established outward movement of the intracellular segments of these helices. The conserved proline-bends of the involved helices seem to constitute the pivots for these vertical seesaw movements (Elling et al., 2006). Such a model, with a considerable induced-fit component comprising a "closing" of the binding-pocket around the small agonist ligand, is in agreement with recent structure-function studies in both the β_2-adrenergic receptor and the M3 muscarinic receptor (Carmine et al., 2004; Kobilka, 2004; Liapakis et al., 2004; Swaminath et al., 2004; Han et al., 2005).

In the present study, we tested the hypothesis that small molecules act as agonists for 7TM receptors by holding TM-VI and -VII in an inwardly bent, proposed active conformation. An engineered metal ion site is employed as an anchor point to tether small, aromatic chelators in the main ligand-binding pocket of the CXCR3 chemokine receptor (Fig. 1) at a position corresponding to the presumed binding site for catecholamine agonists in, for example, the β_2-adrenergic receptor (Shi and Javitch, 2002; Kobilka, 2004). The CXCR3 receptor, which is normally activated by large chemokines such as ITAC (CXCL11) and IP10 (CXCL10), was chosen as a model system because it had previously proven to be particularly robust and well suited for extensive mutational engineering in the main ligand-binding pocket (Rosenkilde et al., 2004). Through mutational analysis combined with molecular modeling and simulations, it is found that the metal ion site anchored chelators act as highly efficacious agonists through establishing second-site, aromatic-aromatic interactions with a Tyr residue on the inner face of TM-VI, TyrVI:16, thereby completing an "aromatic zipper" among TM-III, -VI, and -VII that holds the extracellular segment of especially TM-VI in an inwardly bent, presumed active conformation. The two other components of the proposed aromatic zipper TyrIII:08 and TyrVII:10 are located at the classic anchor-point for monoamines (AspIII:08 in monoamine receptors) and the attachment site for retinal in TM-VII, LysVII:10 (Lys^{296}) in rhodopsin, respectively.

Materials and Methods

Materials. The CXCR3 chemokine ligands CXCL10/IP10 and CXCL11/ITAC were purchased from PeproTech (Rocky Hill, NJ). The metal ion chelator complexes were created by mixing 2,2′-bipyridine (Aldrich Chemical Co., Milwaukee, WI) or 1,10-phenanthrolene with $CuCl_2$ or $ZnCl_2$ in the relation 2:1. Human CXCR3 cDNA was kindly provided by Kuldeep Neote (Pfizer, Groton, CT). The Gα6qi4myr construct was kindly provided by Evi Kostenis (University of Bonn, Bonn, Germany).

Site-Directed Mutagenesis. Point mutations were introduced in the receptors by the polymerase chain reaction overlap extension

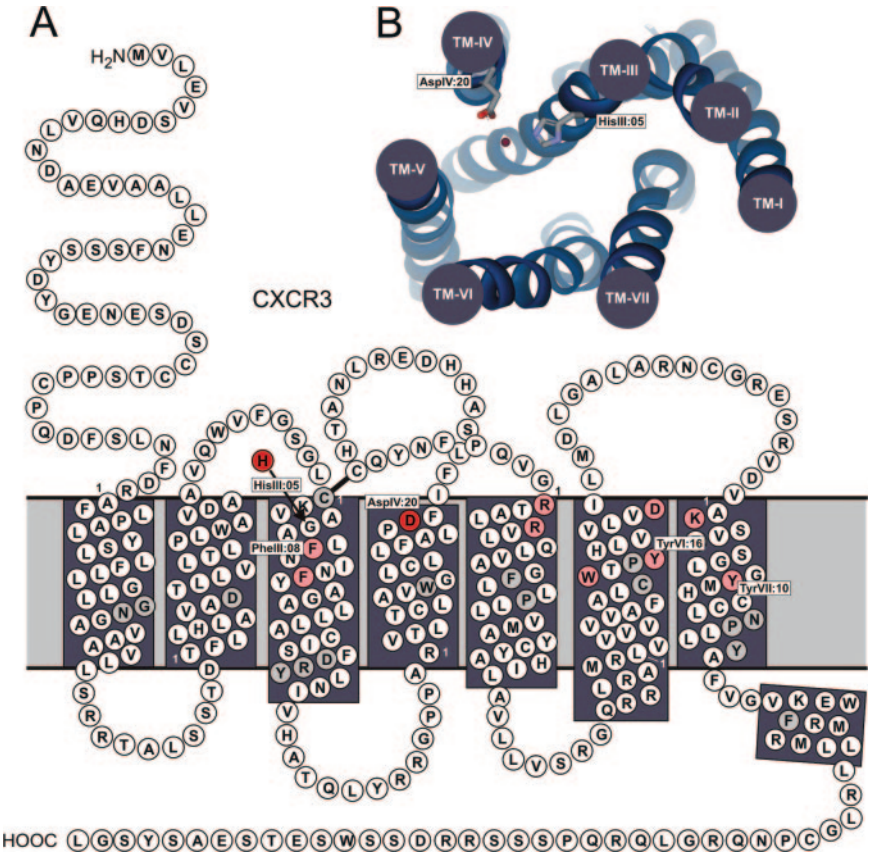

Fig. 1. The CXCR3 receptor used for metal ion site engineering and molecular modeling and simulation. A, serpentine model of the CXCR3 receptor. Highlighted in dark red are the two residues comprising the anchoring metal ion site: the His introduced instead of GlyIII:05 (Gly^{128}) and the endogenous AspIV:20 (Asp^{186}). Highlighted in light red are various residues that are mutated to try to identify potential metal ion site partners, second-site interaction sites for the aromatic chelators, or supporting "aromatic zipper" residues (see Figs. 6 and 7). The position of PheIII:08 (Phe^{131}), TyrVI:16 (Tyr^{271}), and TyrVII:10 (Tyr^{308}) are specifically indicated. In gray are highlighted conserved fingerprint residues, which characterize the individual transmembrane segments. B, a molecular model of the seven helical bundle of the basic [HisIII:08]-CXCR3 receptor construct built over the X-ray structure of the inactive, dark state of rhodopsin (Palczewski et al., 2000) in blue solid ribbon format. The two residues that, according to the Relibase analysis and molecular modeling, can form an ideal metal ion site in the inactive form of the receptor: HisIII:05 and AspIV:20 are shown in stick models as ligands for a metal ion (magenta sphere) docked into the receptor model (see text for details).

technique. All reactions were carried out using the *Pfu* polymerase (Stratagene, La Jolla, CA) under conditions recommended by the manufacturer. The generated mutations were cloned into the eukaryotic expression vector pcDNA3+. The mutations were verified by DNA sequencing (MWG Biotech, High Point, NC).

Transfections and Cell Culture. COS-7 cells were grown at 10% CO_2 and 37°C in Dulbecco's modified Eagle's medium with GlutaMAX (Invitrogen, Carlsbad, CA) adjusted with 10% fetal bovine serum, 180 U/ml penicillin, and 45 ug/ml streptomycin. Transfection of the COS-7 cells was performed by the calcium phosphate precipitation method (Rosenkilde et al., 1999).

Phosphatidyl Inositol Assay (Phosphatidyl Inositol Turnover). COS-7 cells (6×10^6 cells/flask) were transfected with 20 μg of receptor cDNA in addition to 30 μg of the promiscuous chimeric G-protein Gα6qi4myr (Kostenis et al., 1998), which turns the Gα_i-coupled signaling of the CXCR3 receptor into the Gα_q pathway [i.e., phospholipase C activation measured as phosphatidyl inositol turnover (Berridge et al., 1983)]. One day after transfection, the cells were seeded into wells (2.5×10^4 cells/well) and incubated for 24 h with 2 μCi of [*myo*-^{3}H]inositol (Amersham Pharmacia Biotech) in 0.4 ml of growth medium per well. Cells were washed twice in 20 mM HEPES, pH 7.4, supplemented with 140 mM NaCl, 5 mM KCl, 1 mM $MgSO_4$, 1 mM $CaCl_2$, 10 mM glucose, and 0.05% (w/v) bovine serum albumin; and were incubated in 0.4 ml of buffer supplemented with 10 mM LiCl at 37°C for 90 min in the presence of ligands. Cells were extracted by addition of 1 ml of 10 mM Formic acid to each well followed by incubation on ice for 30 min. The generated [^{3}H]inositol phosphates were purified on AG 1-X8 anion exchange resin (Bio-Rad Laboratories, Hercules, CA) (Rosenkilde et al., 1999). Determinations were made in duplicates.

Calculations. EC_{50} and potency values were determined by nonlinear regression using Prism 3.0 software (GraphPad Software, San Diego, CA).

Molecular Modeling and Simulations. Molecular homology models of the [HisIII:05]CXCR3 receptor were built over the X-ray structure of the inactive state of rhodopsin using the software package MODELLER (http://salilab.org/modeller/) as described in detail in the Supplementary Material. Relibase (http://relibase.ebi.ac.uk; Hendlich et al., 2003), a database of high-resolution experimental protein-ligand complexes, was used to design a silent, anchoring metal ion site between a His residue introduced at position III:05 (Gly^{128}–His) and the natural Asp residue at position IV:20 (Asp^{186}). A Zn(II) metal ion as well as an aromatic metal ion chelator (i.e., bipyridine or phenanthroline) were docked into the molecular model, which was subjected to energy minimizations. Models of the presumed active receptor conformation were generated by a Monte Carlo simulation annealing protocol (Li and Scheraga, 1987) using the NOE functionality of CHARMM with distance constraints for the extracellular segments of TM-III, TM-VI, and TM-VII corresponding to Cβ-Cβ distances defined by the previously described activating metal ion site originally constructed between positions III:08, VI:20, and VII:06 in the β_2-adrenergic receptor (Elling et al., 2006), as well as distance constraints of the intracellular segments of these helices as defined by the EPR analysis of the movements in rhodopsin during activation (Hubbell et al., 2003), as described in detail in the supplementary material.

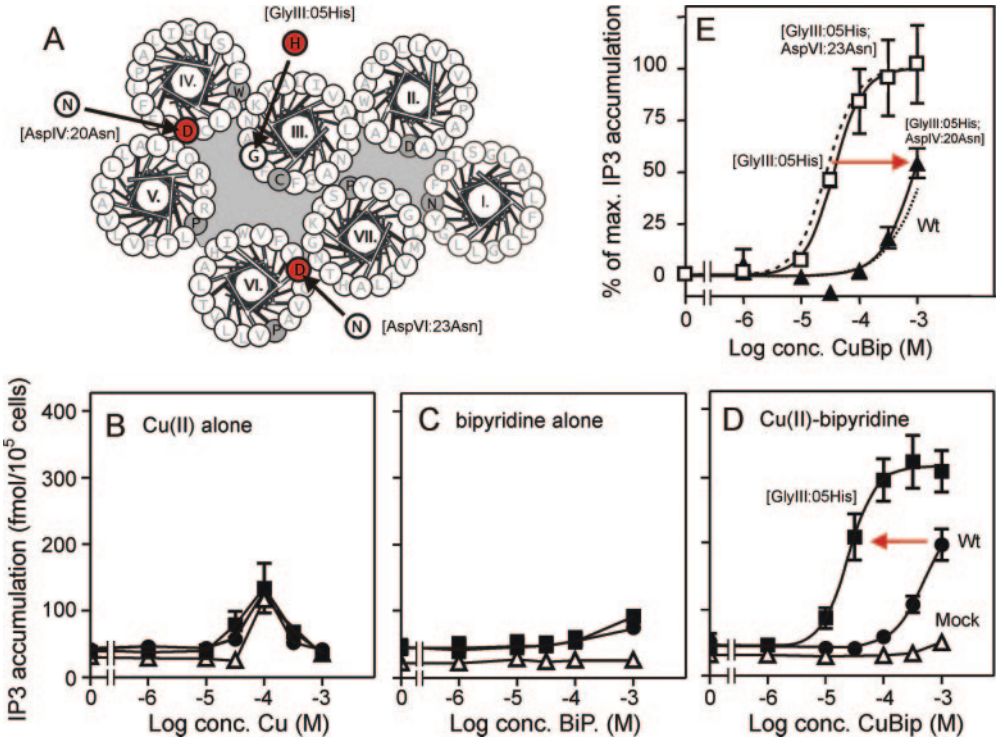

Fig. 2. Construction of an interhelical, bidentate metal ion binding site between position III:05 and position IV:20 in the CXCR3 chemokine receptor. A, helical wheel diagram of the CXCR3 receptor as seen from the extracellular side. In gray are highlighted the "fingerprint" residues in each transmembrane helix. It should be noted that this schematic format gives a misleading picture of the actual distances between residues, especially between helices (Fig. 1B). GlyIII:05 was substituted with His (highlighted in red)—as a potential metal ion binding residue—producing [GlyIII:05His]-CXCR3. Effect of free Cu(II) ions (B), the bipyridine chelator (BIP) alone (C), and the Cu-bipyridine metal ion chelator complex (D) on signal transduction as measured by inositol trisphosphate (IP3) accumulation in control cells (△) and in COS-7 cells transiently transfected with either the CXCR3 wild-type (●), the [GlyIII:05His]-CXCR3 construct (■), or mock-transfected cells (△). In B to D, total production of IP3 is indicated in femtomoles per 10^5 cells. E, mutational analysis of the endogenous metal ion site partner for the introduced HisIII:08 in the CXCR3 receptor. AspIV:20 or AspVI:23 were individually substituted by Asn producing [GlyIII:05His;AspIV:20Asn]-CXCR3 (▲) and [GlyIII:05His;AspVI:23Asn] (□). Dose-response curves for Cu(II)-bipyridine stimulation of IP3 production in transiently transfected COS-7 cells are shown. The broken line indicates the effect in the [GlyIII:05His] background construct, and the dotted line indicates the effect in the wild-type receptor.

Results

Construction of an Anchoring Metal Ion Site between TM-III and -IV. In the β_2-adrenergic receptor, the monoamine agonists use an Asp in position III:08 as a counter-ion attachment point (Strader et al., 1991; Shi and Javitch, 2002; Kobilka, 2004). In the CXCR3 receptor we chose position III:05 (residue 128) one helical turn "above" III:08 as the starting point for the construction of an anchoring metal ion site (Figs. 1 and 2A). Computational chemistry analysis of the geometry of a large number of experimentally characterized metal ion sites compiled in Relibase (Hendlich et al., 2003) revealed that a His residue introduced at this position could make a perfect metal ion site [i.e., with respect to angles and distances] with the naturally occurring AspIV:20 (Asp^{186}) located on the opposing face of TM-IV with both residues in their preferred rotameric states (see Supporting Data) (Fig. 1B). Position IV:20 is known to be readily accessible for small molecule nonpeptide ligand interactions, as extensively studied in both the CXCR3 and CXCR4 receptors (Gerlach et al., 2003; Rosenkilde et al., 2004).

In accordance with the fact that HisIII:05 and AspIV:20 can form the metal ion site already in the inactive receptor conformation, the free metal ions Zn(II) or Cu(II) had no agonistic effect in the [HisIII:05]-CXCR3 construct (Fig. 2B, Table 1). Likewise, the chelators bipyridine and phenanthrolene had no agonistic property on their own in neither the wild-type nor the [HisIII:05]-CXCR3 construct (Fig. 2C, Table 1). It is noteworthy that when presented in complex with metal ions, the aromatic chelators acted as high-potency and high-efficacy agonists in the [HisIII:05]-CXCR3 construct (Fig. 2D, Table 1). Highest potency (8.0 μM) was displayed by Cu(II)-phenanthrolene, corresponding to a 38-fold increase compared with the wild-type receptor (Table 1). In the [HisIII:05]-CXCR3 construct, the endogenous chemokines ITAC and IP10 displayed an E_{max} that was ~40% of that obtained in the wild-type CXCR3 receptor, whereas in the [HisIII:05]-CXCR3 construct, the maximal efficacy of the metal ion complexes was 1.5- to 1.8-fold *superior* to that of even the most efficacious endogenous chemokine, ITAC (CXCL11), as shown for Cu(II)-bipyridine in Fig. 3A (Table 1). No potentiating or inhibitory effect was observed during coadministration of ITAC and Cu(II)-bipyridine but instead an additive effect, where administration of Cu(II)-bipyridine simply brought the signaling efficacy of the [HisIII:05]-CXCR3 construct up to the higher E_{max} observed for Cu(II)-bipyridine alone (Fig. 3, B and C). It can be argued

TABLE 1

Potencies and efficacies of different metal ion chelator complexes on wild-type and His III:05 (His^{128})-CXCR3

The effect of the chemokines ITAC and IP10, the metal ion chelator complexes, the chelators, and the metal ions were measured by the phosphatidyl inositol turnover experiment in transiently transfected COS-7 cells. *n* refers to the number of experiments. ± values are S.E.M.

	Wild-Type CXCR3				His III:05 (His^{128})-CXCR3					
	Log EC_{50}	EC_{50}	*n*	E_{max}	Log EC_{50}	EC_{50}	*n*	F_{inc}	E_{max}	E_{max}
		nM		*fmol / 10^5 cells*		*nM*		*-fold*	*fmol / 10^5 cells*	%
Endogenous chemokines										
ITAC (CXCL11)	−8.8 ± 0.08	1.7	23	544 ± 67	−7.8 ± 0.09	15	16	0.11	215 ± 31	100
IP10 (CXCL10)	−8.0 ± 0.10	11	21	407 ± 46	−6.9 ± 0.22	163	14	0.07	163 ± 32	72
Metal ion chelator complexes										
Cu(II)-Bip	−3.0 ± 0.09	973[a]	19	NE	−4.7 ± 0.11	22	18	44	347 ± 32	171
Zn(II)-Bip	−2.9 ± 0.01	1169[a]	9	NE	−4.3 ± 0.08	53	15	22	313 ± 33	153
Cu(II)-Phen	−3.5 ± 0.12	302[a]	8	NE	−5.1 ± 0.04	8.0	10	38	327 ± 60	161
Zn(II)-Phen	−3.2 ± 0.18	595[a]	6	NE	−4.7 ± 0.05	21	8	29	300 ± 53	146
Metal ions										
Cu (II)	<−2	>10,000	4	NE	<−2	>10,000	6		NE	NE
Zn (II)	<−2	>10,000	4	NE	<−2	>10,000	6		NE	NE

E_{max}, maximum stimulation; F_{inc}, -fold increase in potency for each ligand on His III:05-CXCR3 compared with wild-type CXCR3; E_{max} (%), average specific efficacy of a given ligand where 100% equals the maximal specific ITAC stimulation on His III:05-CXCR3; Bip, bipyridine; Phen, phenanthrolene; NE, no detectable E_{max}.

[a] The EC_{50} was estimated by a nonlinear regression using the sigmoidal dose-response algorithm in GraphPad Prism with a constant Hill coefficient of 1.5 corresponding to the Hill coefficient of the metal ion chelator complexes on His III:05 CXCR3.

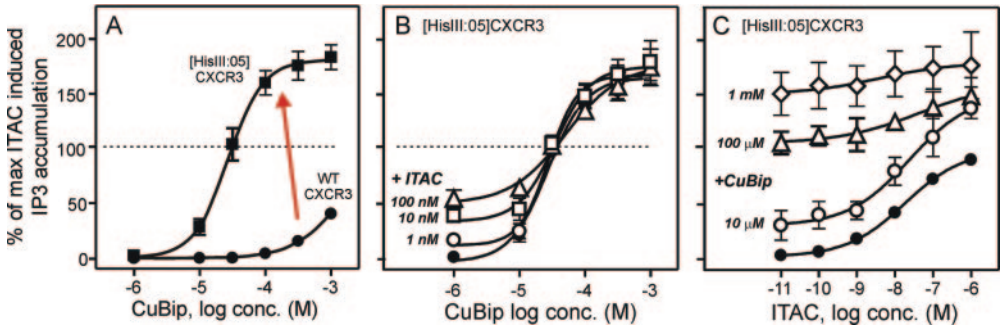

Fig. 3. Comparison of the effect of Cu(II)-bipipyridine and ITAC and coadministration of the two agonists in the [GlyIII:05His]-CXCR3 receptor. A, IP3 production in response to Cu(II)-bipyridine as percent of the maximal IP3 production observed under stimulation with the endogenous chemokine, ITAC, in the wild-type CXCR3 receptor (●) and in the [GlyIII:05His]-CXCR3 construct (■). The red arrow indicates the effect of the introduction of the His residue at position III:05. B, dose-response curves for Cu(II)-bipyridine in the absence (●) and presence of 1 nM (○), 10 nM (□), and 100 nM (△) of ITAC. C, dose-response curves for ITAC in the absence (●) and presence of 10 μM (○), 100 μM (△), and 1 mM (□) of Cu(II)-bipyridine. The two agonists were administered simultaneously (n = 3–4).

that this supports a model where ITAC and Cu(II)-bipyridine function as coagonists in an unconventional type of allosteric mechanism (Schwartz and Holst, 2006).

Ala substitution of AspIV:20 confirmed that this residue was indeed the metal ion binding partner for HisIII:05 in the [HisIII:05]-CXCR3 construct as reflected in the 40-fold rightward shift in the dose-response curve for Cu(II)-bipyridine (Fig. 2E, Table 2). As a control, AspVI:23 could be mutated without any effect of the agonist potency of Cu(II)-bipyridine (Fig. 2E).

Identification of Second-Site Interactions for the Aromatic Chelators. The high efficacy and potency of the metal ion chelator complexes compared with the free metal ions indicate that the chelators make significant second-site interactions in the active receptor conformation. To identify such interaction points, we performed a systematic mutational analysis of possible interaction partners at the inner faces of TM-III, -V, -VI, and -VII in the [HisIII:05]-CXCR3 background (Fig. 4, Tables 2 and 3). No effect was observed by substitution of the potential cation-π interaction partners ArgV:01, ArgV:05, and LysVII:02 (Fig. 4, B and C; Table 2). In addition, only a very minor effect was observed by Ala substitution of the potential aromatic-aromatic interaction partners, TrpVI:13 and PheIII:12—both located relatively deep in the pocket (Fig. 4D, Table 2). In contrast, Ala substitution of TyrVI:16 (Tyr^{271}) shifted the dose-response curve for Cu(II)-bipyridine 37-fold to the right (Fig. 4E). Likewise, introduction of either an aliphatic, hydrophobic Leu residue or a polar Asn residue at this position impaired the potency of Cu(II)-bipyridine by 58- and 31-fold, respectively (Table 2). It is noteworthy that the potency of the chemokine ITAC was in fact *improved* 2.5- to 10-fold by these three substitutions of TyrVI:16, indicating that the mutations did not cause general harm to the receptor (Table 2). Substitution of TyrVI:16 with either a Phe or a His residue had only minor effects on the potency of Cu(II)-bipyridine (Table 2).

These results indicate that the bipyridine or phenanthrolene chelators in complex with metal ions obtain their high potency and agonist efficacy in the [HisIII:05]-CXCR3 construct though establishment of a second-site interaction with TyrVI:16 on the opposing face of TM-VI—conceivably through an aromatic-aromatic interaction.

In molecular models of the [HisIII:05]-CXCR3 receptor built over the X-ray structure of the inactive conformation of rhodopsin, even the closest distance between the bipyridine moiety tethered to HisIII:05 through the metal ion and the side-chain of TyrVI:16 (5.6 Å) is nevertheless too long to correspond to an aromatic-aromatic interaction. However, according to the recently proposed global toggle switch activation model for 7TM receptors, the extracellular segment of TM-VI will during activation of the receptor swing or tilt inward toward TM-III (Elling et al., 2006).

Molecular Simulation of the Activation Mechanism of [HisIII05]-CXCR3. To mimic the proposed vertical seesaw movements of TM-VI and TM-VII (Elling et al., 2006), the molecular model of the [HisIII:05]-CXCR3 receptor was subjected to molecular simulations (see Supplementary Material for details) (Fig. 5). To encourage inward movement of the extracellular segments of TM-VI and TM-VII, the Cβ-Cβ distances for the previously constructed activating metal ion site between positions III:08, VI:16, and VII:06 in the β_2-adrenergic receptor (Elling et al., 2006), were used as NOE distance constraints during the molecular simulations. Moreover, to make the intracellular segments of these helices move outward, the distance constraints provided by the EPR analysis of the activation mechanism for rhodopsin were applied to the intracellular segments of TM-VI and -VII (Hubbell et al., 2003) (Fig. 5). The root-mean-square devia-

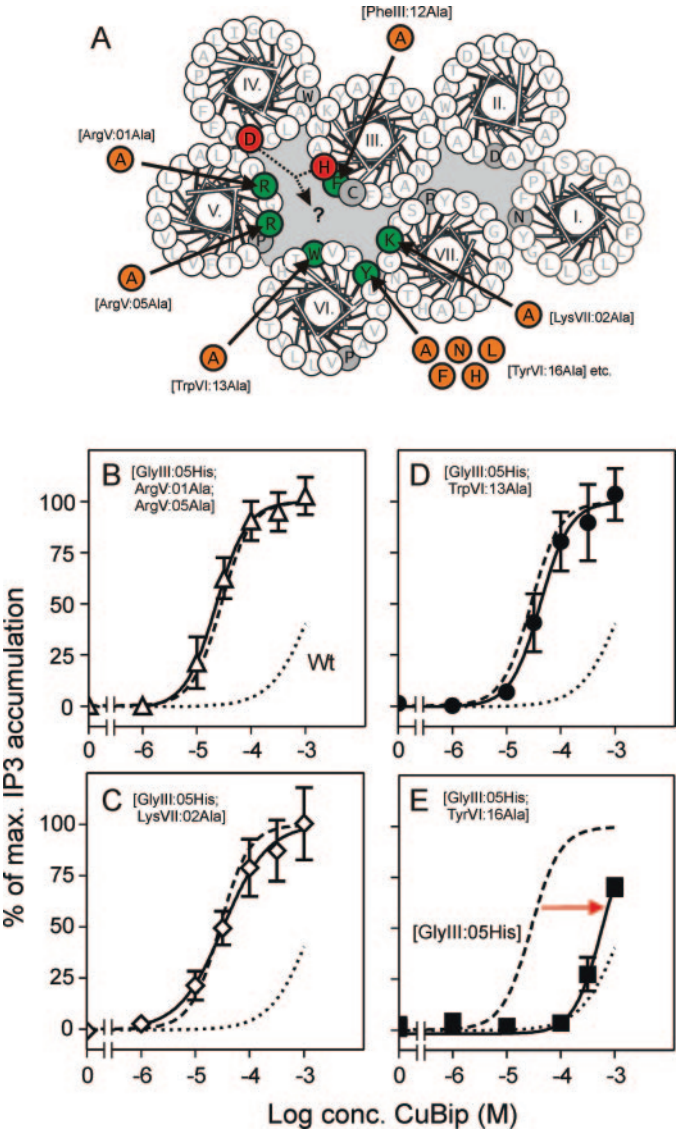

Fig. 4. Identification of residues involved in second-site interactions and required for the aromatic chelators in complex with metal ions to act as agonists in the [GlyIII:05His]-CXCR3 receptor. A, helical wheel diagram of the [GlyIII:05His]-CXCR3 receptor. AspIV:20 and HisIII:05, which are presumed to make an anchoring, interhelical bidentate metal ion site (see Fig. 1) are highlighted in red. Residues, which were mutated to identify the second-site interaction for the aromatic chelators in the [GlyIII:05His]-CXCR3 receptor, are highlighted in green, and the residues, which were introduced at the various positions are indicated in orange. B–E, dose-response curves for Cu(II)-bipyridine in selected receptor constructs. B, [GlyIII:05His;ArgV:01Ala;-ArgV:05Ala]-CXCR3 (△). C, [GlyIII:05His;LysVII:02Ala]-CXCR3 (◇). D, [GlyIII:05His;TrpVI:13Ala]-CXCR3 (●). E, [GlyIII:05His;TyrVI:16Ala]-CXCR3 (■). Also shown for comparison in each panel are the dose-response curve for Cu(II)-bipyridine is the CXCR3 wild-type receptor (dotted curve) and the [GlyIII:05His]-CXCR3 background construct (hatched curve) as determined in transiently transfected COS-7 cells. The red arrow indicates the 37-fold decrease in potency for the Cu(II)-bipyridine as a result of Ala-substitution of TyrVI:16.

tion (RMSD) for the trajectories were followed during the simulation. As shown in Fig. 5B, after 4.000 Monte Carlo steps, the simulation converged toward a stable conformation, which had an RMSD of ~2 Å relative to the starting, inactive CXCR3 conformation. Likewise, the total energy of the system demonstrates a stable simulation with decreasing energies of the system that converge to a steady level halfway through the simulation.

As a result of the inward movement of the extracellular segment of TM-VI during the molecular simulation, the distance between the lower ring of the bipyridine chelator and the phenol ring of TyrVI:16 shortened to ~3 Å, which is compatible with a close aromatic-aromatic interaction (Fig. 5C). As shown in Fig. 6, A and B, during the proposed activation process, the side chain of TyrVI:16 moves into a position where it interacts closely not only with the lower ring of the pyridine ligand but also with the side chain of PheIII:08 (Phe^{131}). The opposite side of PheIII:08, on the other hand, interacts closely with TyrVII:10 (Tyr^{308}) (Fig. 6, A and B).

Thus, the molecular modeling and simulations indicate that the aromatic metal ion chelator from its tethered position in the bidentate metal ion site between HisIII:05 and AspIV:20 acts as an agonist by establishing a second-site, aromatic-aromatic interaction with TyrVI:16, which presumably holds TM-VI in its active, inwardly bent conformation. Importantly, the molecular simulations also indicate that the aromatic chelator and TyrVI:16 together with PheIII:08 and TyrVII:10 form an extended "aromatic zipper" between the extracellular segments of TM-III, TM-VI, and TM-VII.

Mutational Analysis of the Proposed "Aromatic Zipper." Substitution of PheIII:08 in the [HisIII:05]-CXCR3 background shifted the dose-response curves for all the metal

TABLE 2

Mutational analysis of residues potentially involved in metal site or as second site interaction

The effect of CuBip and ITAC were measured by the phosphatidyl inositol turnover experiments in transiently transfected COS-7 cells. *n* refers to the number of experiments. ± values are S.E.M.

		Cu(II)-Bipyridine						ITAC					
		Log EC_{50}	EC_{50}	*n*	F_{dec}	E_{max}	E_{max}	Log EC_{50}	EC_{50}	F_{dec}	*n*	E_{max}	E_{max}
			μM		*-fold*	*fmol / 10⁵ cells*	*%*		*nM*	*-fold*		*fmol / 10⁵ cells*	*%*
III:05	G128H	−4.7 ± 0.11	22	18	1.0	347 ± 32	162	−7.8 ± 0.09	15	1.0	16	215 ± 31	36
Background													
III:08	F131A	−2.8 ± 0.09	1415[a]	4	64	NE	NE	−7.5 ± 0.39	35	2.4	3	72 ± 10	8
III:12	F135L	−4.3 ± 0.23	55	3	2.5	247 ± 29	172	−8.1 ± 0.14	8.3	0.57	3	144 ± 28	22
IV:20	D186N	−3.1 ± 0.43	885[a]	8	40	NE	NE	−8.0 ± 0.20	9	0.6	8	67 ± 6.9	7
EC2	H202A	−4.2 ± 0.27	58	3	2.6	153 ± 4.4	180	−7.8 ± 0.13	17	1.2	3	85 ± 9.6	11
V:01; V:05	R208A; R212A	−4.9 ± 0.05	12	4	0.22	236 ± 60	259	−7.8 ± 0.36	15	1.1	4	91 ± 14	12
V:05	R212H	−4.7 ± 0.05	19	3	0.85	526 ± 122	227	−7.8 ± 0.03	16	1.1	2	232 ± 33	39
VI:13	W268A	−4.3 ± 0.08	50	5	2.3	313 ± 68	460	−7.6 ± 0.18	27	1.9	6	68 ± 11	7
VI:16	Y271A	−3.1 ± 0.21	794[a]	4	37	NE	NE	−8.8 ± 0.20	1.7	0.12	3	43 ± 1.8	2.5
VI:16	Y271L	−2.9 ± 0.36	1278[a]	4	58	NE	NE	−8.9 ± 0.18	1.3	0.09	4	50 ± 3.0	3.9
VI:16	Y271N	−3.2 ± 0.06	693[a]	3	31	NE	NE	−8.3 ± 0.38	5.6	0.39	3	39 ± 2.9	1.8
VI:16	Y271F	−4.3 ± 0.05	51	3	2.3	263 ± 34	163	−8.1 ± 0.15	7.6	0.52	3	161 ± 37	25
VI:16	Y271H	−4.0 ± 0.03	108	5	4.9	196 ± 29	190	−8.0 ± 0.28	9.6	0.66	5	103 ± 22	14
VI:23	D278N	−4.3 ± 0.12	55	6	2.5	195 ± 31	267	−7.9 ± 0.02	13	0.88	6	73 ± 14	8
VII:02	K300A	−4.7 ± 0.09	20	4	0.90	151 ± 17	150	−8.4 ± 0.05	4.2	0.29	3	101 ± 12	14
VII:10	Y308A	−3.2 ± 0.45	631	3	29	NE	NE	−8.1 ± 0.22	7.4	0.21	3	83 ± 40	10

F_{dec}, decrease in potency for CuBip and ITAC on a given mutation compared with His III:05-CXCR3 (background); E_{max}, maximal stimulation of each ligand; E_{max} (%), for Cu(II)-bipyridine refers to the efficacy of Cu(II)-bipyridine compared with ITAC. E_{max} (%), for ITAC refers to the efficacy on each mutation compared with wild-type CXCR3; NE, no detectable E_{max}.

[a] The EC_{50} was estimated by a nonlinear regression using the sigmoidal dose-response algorithm in GraphPad Prism with a constant Hill coefficient of 1.5 corresponding to the Hill coefficient of Cu(II)-bipyridine on His III:05 CXCR3.

TABLE 3

Comparison of Cu(II) and Zn(II) in complex with bipyridine and Cu(II) in complex with phenanthrolene in respect of residues potentially involved in metal site or as second site interaction

The effect of the metal chelator complexes were measured by the phosphatidyl inositol turnover experiments in transiently transfected COS-7 cells. *n* refers to the number of experiments. ± values are S.E.M.

		Cu(II)-Bipyridine				Zn(II)-Bipyridine				Cu(II)-Phenanthroline			
		EC_{50}	K_d	*n*	$F_{dec.}$	EC_{50}	K_d	*n*	$F_{dec.}$	EC_{50}	K_d	*n*	$F_{dec.}$
			μM		*-fold*		*μM*		*-fold*		*nM*		*-fold*
III:05	G128H	−4.7 ± 0.11	22	18	1.0	−4.3 ± 0.08	53	15	1.0	−4.7 ± 0.05	21	8	1.0
Background													
III:08	F131A	−2.8 ± 0.09	1415[a]	4	64	−3.0 ± 0.15	971[a]	6	18	−3.0 ± 0.13	989[a]	6	47
IV:20	D186N	−3.1 ± 0.43	885[a]	8	40	−2.9 ± 0.31	1240[a]	4	24	−3.6 ± 0.14	241[a]	4	12
V:01; V:05	R208A;R212A	−4.9 ± 0.04	12	4	0.55	−4.5 ± 0.08	29	3	0.55	−5.1 ± 0.15	7.9	3	0.38
VI:13	W268A	−4.3 ± 0.08	50	5	2.3	−3.7 ± 0.24	190	4	3.6	−4.5 ± 0.08	33	6	1.6
VI:16	Y271A	−3.1 ± 0.21	812[a]	4	37	−2.9 ± 0.27	1278[a]	3	24	−3.4 ± 0.02	433[a]	3	21
VI:23	D278N	−4.3 ± 0.12	55	6	2.5	−3.7 ± 0.16	212	3	4.0	−4.5 ± 0.04	35	4	1.7
VII:02	K300A	−4.7 ± 0.09	20	4	0.90	−4.3 ± 0.07	45	3	0.86	−5.1 ± 0.07	7.8	3	0.37
VII:10	Y308A	−3.2 ± 0.45	651[a]	3	29	−3.2 ± 0.70	568[a]	3	11	−3.4 ± 0.07	400[a]	3	19

F_{dec}, decrease in potency for each ligand on a given mutation compared with His III:05-CXCR3 (background).

[a] The EC_{50} was estimated by a nonlinear regression using the sigmoidal dose-response algorithm in GraphPad Prism with a constant Hill coefficient of 1.5 corresponding to the Hill coefficient of the metal ion chelator complexes on His III:05 CXCR3.

ion chelator complexes 18- to 124-fold to the right compared with the wild-type receptor (Fig. 7B) (Tables 2 and 3). It is noteworthy that the PheIII:08 substitution had only a minimal (2.4-fold) effect on the potency of the endogenous chemokine (Table 2). Thus, PheIII:08 is essential for the activation of the metal ion site engineered CXCR3 receptor by metal ion chelator complexes, although this residue according to the molecular models is not in direct contact with the ligand (Fig.

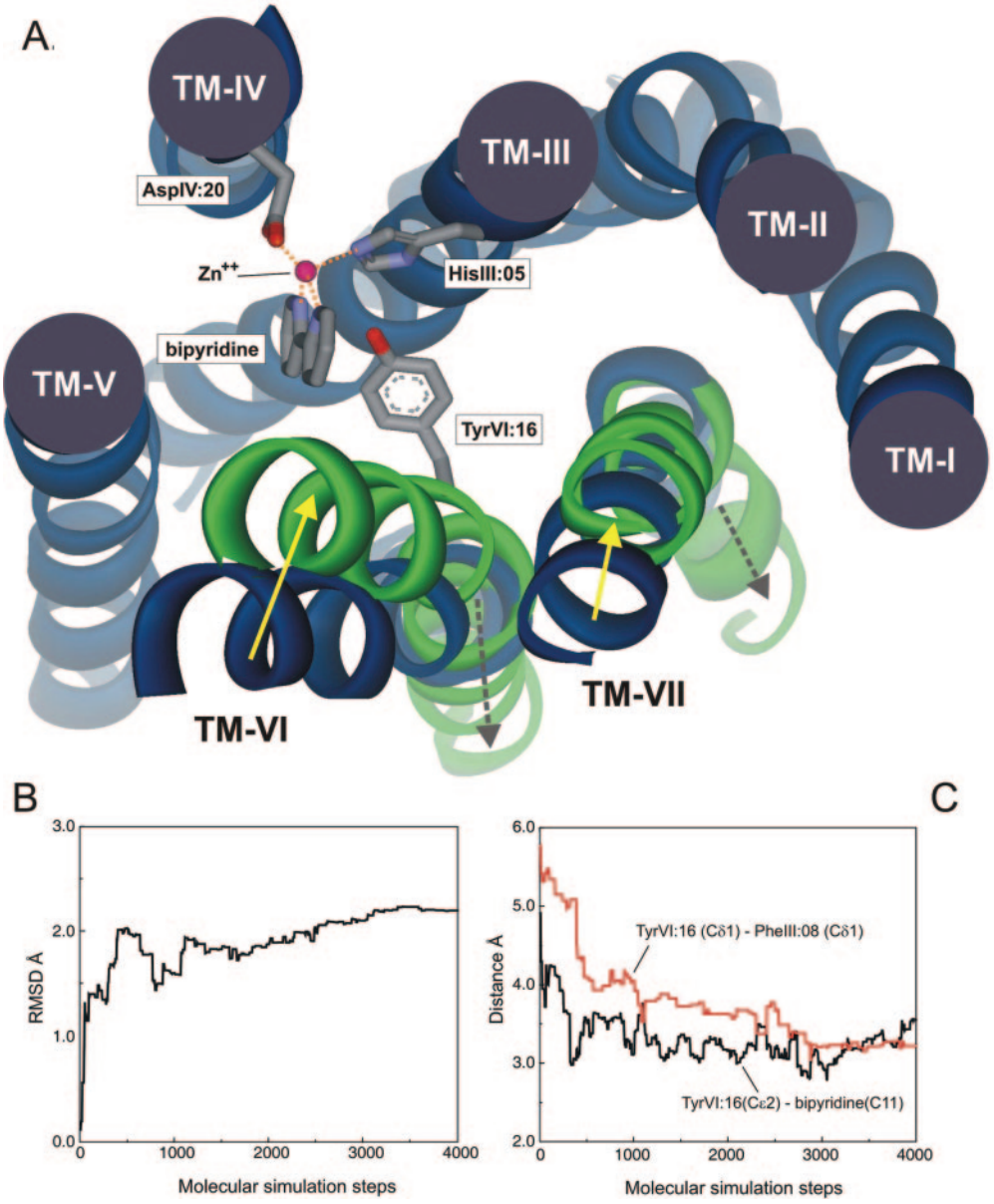

Fig. 5. Molecular modeling and simulation of the presumed activation process of the Zn(II)-bipyridine complex in the [GlyIII:05His]-CXCR3 receptor construct. A, Zn(II) and bipyridine docked into a molecular model of the seven helical bundle of the [GlyIII:05His]-CXCR3 receptor construct built over the X-ray structure of the inactive, dark state of rhodopsin (Palczewski et al., 2000) shown in blue solid ribbon format. The red dotted lines indicate the presumed tetrahedral coordination of the zinc ion (magenta ball) by the carboxyl group of AspIV:20, the imidazole side-chain of HisIII:05 and by the two nitrogens of the bipyridine moiety. The molecular model was subjected to Monte Carlo molecular simulation (see Supplementary Materials for details), during which NOE distance constraints were applied to the Cβ-Cβ distances between positions III:08, VI:16, and VII:06 in the extracellular segments of these helices to try to satisfy the distance constraints of activating metal ion sites previously constructed in the β_2-adrenergic receptor (Elling et al., 2006). Conversely, NOE distance constraints were applied to the intracellular segments of TM-VI relative to TM-III and TM-V as well as TM-VII relative to TM-II and -III to try to account for the movements of these helices during activation of rhodopsin as identified by the EPR analysis (Hubbell et al., 2003). The backbone of TM-I through TM-V was not allowed to move during these molecular simulation experiments. In green ribbons are shown the position of TM-VI and TM-VII in a presumed active conformation after the molecular simulation of the activation process. TyrVI:16 on the inner face of TM-VI, which by the mutagenesis was indicated to be the major second-site interaction point for the metal ion chelator complexes (Fig. 2), is highlighted. The yellow arrows indicate the proposed inward movement of the extracellular segments of TM-VI and TM-VII, whereas hatched dark arrows indicate the opposite, outward movement of the intracellular segments of these helices. B, RMSD between the inactive and the activated CXCR3 receptor conformation measured during the molecular simulation procedure. C, in black is shown the distance between the side-chain of TyrVI:16 (aromatic atom CE1) and the lower ring of the bipyridine ligand (atom C11) and in red is shown the distance between the side-chain of TyrVI:16 (aromatic atom CD1) and the phenyl side-chain of PheIII:08 (aromatic atom CD2) (in red) measured throughout the molecular simulation.

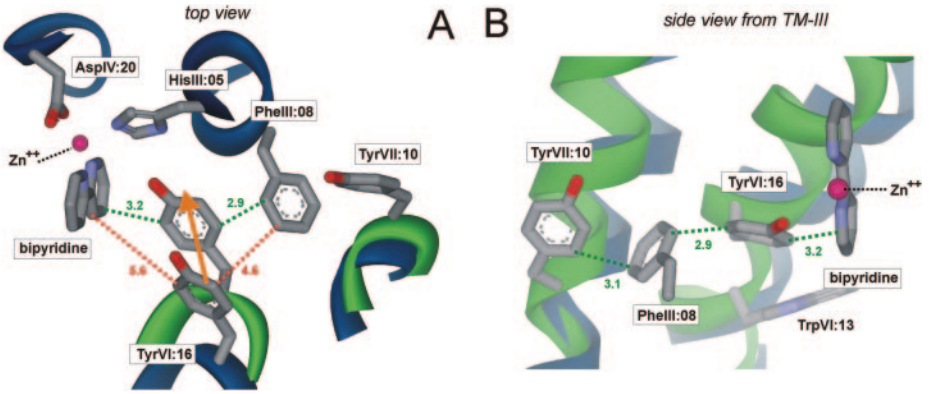

Fig. 6. The "aromatic zipper" that is proposed to be responsible for the activation of the [GlyIII:05His]-CXCR3 receptor by Zn(II)-bipyridine. A, top view of the aromatic zipper shown in both the inactive state (green ribbon and red distances) and the proposed active state at the end of the molecular simulation (green ribbon and green distances—see text for details). The orange arrow indicates the direction of the proposed inward movement of TM-VI through which TyrVI:20 is brought into a position between the metal ion site anchored bipyridine moiety and the side chain of PheIII:08 during the activation process. TyrVII:10, which completes the presumed aromatic zipper on the opposite side of PheIII:08, is also shown. B, side view of the aromatic zipper as seen from TM-III, which, together with TM-IV, has been omitted except for the side-chain of PheIII:08.

6).[1] Likewise, even the side chain of TyrVII:10, which completes the proposed "aromatic zipper" at the opposite end of the main ligand-binding pocket—compared with the bipyridine moiety—was also found to be highly important for the activation mechanism, because Ala-substitution of TyrVII:10 shifted the dose-response curves for the metal ion chelator complexes 11- to 50–100-fold to the right (Fig. 7C, Table 2). In the case of TyrVII:10, the dependence upon the proposed aromatic zipper was also restricted to the aromatic chelator agonists and not the chemokine proteins (Table 2).

In conclusion, the mutational analysis indicates that all four components of the "aromatic zipper" across the main ligand-binding crevice are required to hold the receptor in its active conformation when activated by the small aromatic chelators. The interaction between the metal ion site-tethered bipyridine moiety and TyrVI:16 is not in itself sufficient to stabilize the active receptor conformation because the backing of TyrVI:16 by PheIII:08 is essential (Fig. 7B). However, not even the stabilization of TyrVI:16 by PheIII:08 is enough, as indicated by the clear effect of Ala-substitution of TyrVII:10 located "behind" both TyrVI:16 and PheIII:08 (Fig. 7C). That is, these aromatic residues are required when the small aromatic chelators bipyridine or phenanthrolene act as agonists. In contrast, the large chemokine proteins can activate the receptor totally independently on these residues located relatively deep in the main ligand-binding pocket of the CXCR3 receptor. Moreover, the lack of appreciable constitutive activity of the CXCR3 receptor indicates that the interdigitation of the endogenous three aromatic side chains of TyrVI:16, PheIII:08, and TyrVII:10 is not strong enough to hold the receptor in its active conformation without the presence of the metal ion site tethered aromatic chelator.

Discussion

In rhodopsin-like 7TM receptors, the binding sites for small molecule ligands—agonists as well as antagonists—have repeatedly been described to be located in the main ligand-binding pocket between the extracellular segments of the seven helical bundle, with special focus on the interfaces of TM-III, -V, -VI, and -VII (Schwartz et al., 1995; Schwartz and Holst, 2002; Shi and Javitch, 2002). However, although various differences have been described between agonist and antagonist interactions in specific cases, the general molecular mechanism (which, for some compounds, leads to agonism and for other, perhaps structurally rather similar compounds, instead leads to antagonism) has remained unclear. The results of the present study provides evidence for the notion that compounds that are agonists are those that are able to function as "molecular glue" between the extracellular segments of TM-III, -VI, and -VII in a way that stabilizes an inwardly bent, active conformation of especially TM-VI (Fig. 5). In contrast, compounds that bind in the same pocket but that are not able to hold TM-VI in the correct inwardly bent conformation or even prevent this inward movement of TM-VI and -VII, will then instead be expected to act as antagonists or inverse agonists. The issue that there will be differences between the molecular mechanism of antagonism and inverse agonism is not dealt with here because the present article focuses on agonism.

Small Molecule 7TM Agonists. Residues involved in ligand binding in the β_2-adrenergic receptor—a prototype 7TM receptor—have been identified and studied extensively over the last ~15 years (Strader et al., 1991; Shi and Javitch, 2002; Kobilka, 2004) (Fig. 8a). The key anchoring site for agonists in the β_2-adrenergic receptor—as well as in all other monoamine receptors—is the highly conserved AspIII:08, which functions as a counter ion for the positively charged amine group of the ligand (Strader et al., 1991; Shi and Javitch, 2002). One way to envision the agonist-induced activation process in this receptor would be that a compound such as isoproterenol initially is tethered through long-range, charge-charge interactions with AspIII:08 and is oriented in the binding pocket by hydrogen-bond interactions between the catechol ring and serine residues in TM-V to subsequently make the final, critical interactions with residues on the inner faces of TM-VI, in particular AsnVI:20 and PheVI:17 (Strader et al., 1991; Wieland et al., 1996; Shi and Javitch, 2002; Carmine et al., 2004; Kobilka, 2004; Liapakis et al., 2004) (Fig. 5A). It has recently been proposed that the binding and activation process in the β_2-adrenergic receptor

[1] In our model, the closest distance between bipyridine and PheIII:08 is ~8 Å, and TyrVI:17 is located between. It would require major nonfavorable alterations to the model—or a whole other molecular model—to bring the bipyridine in direct contact with PheIII:08.

has to involved a certain amount of induced fit (Carmine et al., 2004; Kobilka, 2004; Liapakis et al., 2004). However, although isoproterenol is a relatively small agonist, it is still difficult to precisely predict its mode of action. For example, the relative contribution of the various potential hydrogen bond donor/acceptor residues in TM-IV and -V as well as the aromatic residues in TM-VI is still somewhat unclear. In the present study, we have addressed the question of mechanism of action for small molecule agonists by instead making a small, very simple organic compound—bipyridine or phenanthrolene—act as a highly efficacious agonist by tethering it through an anchoring, silent metal ion site at a position corresponding to the β_2-adrenergic agonists binding site between TM-III and -V in a receptor, which normally is activated by large chemokines (Fig. 8). The molecular modeling and simulations as well as mutational analysis indicate that the small aromatic chelators act as agonists by establishing an aromatic-aromatic second site interactions with TyrVI:16 on the opposing face of TM-VI (Figs. 5 and 6). It is noteworthy that this aromatic-aromatic interaction can only be established if the extracellular segment of TM-VI is tilted inward to a position defined by the distance constraints identified by the activating metal ion sites previously built between positions III:08, VI:16, and VII:06 in the β_2-adrenergic receptor (Elling et al., 2006). Interestingly, in the metal ion site-engineered CXCR3 receptor, the chelator and TyrVI:16 form part of an extended aromatic zipper also comprising PheIII:08, which corresponds to the monoamine anchor point, as well as TyrVII:10, which corresponds to the Schiff-base attachment site for retinal in TM-VII of rhodopsin [i.e., LysVII:10 (Lys^{296})]. Not only TyrVI:16 but also PheIII:08 as well as TyrVII:10 are required for the agonist action of the aromatic chelators (i.e., to hold TM-VI and TM-VII in an inwardly bent, active conformation) (Fig. 3).

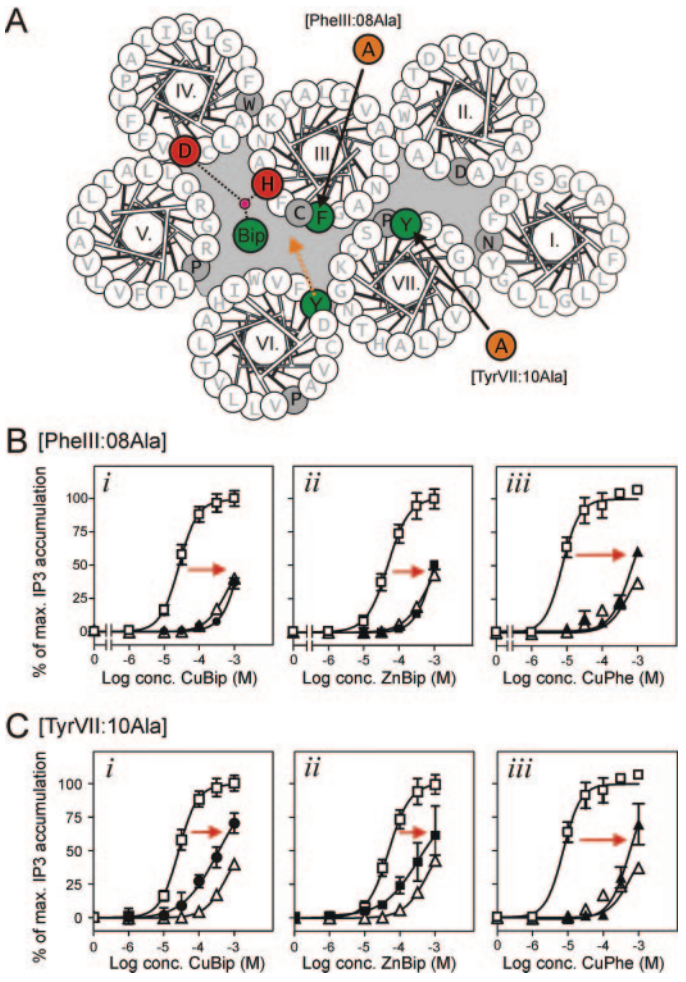

Fig. 7. Mutational characterization of the "aromatic zipper" that, according to the molecular simulations, is proposed to be generated across the main ligand-binding pocket of the [GlyIII:05His]-CXCR3 receptor through the metal ion site guided binding of the chelator. A, helical wheel diagram of the [GlyIII:05His]-CXCR3 receptor. AspIV:20 and HisIII:05, which constitute the anchoring, interhelical metal ion site (see Fig. 1), are highlighted in red. The aromatic chelator—in this case bipyridine—TyrVI:16 (identified as a second site interaction point for the chelator—see Fig. 2), as well as PheIII:08 and TyrVII:10, which were suggested by the molecular simulation to be supporting parts of the aromatic zipper and consequently were subjected to Ala-substitution, are all highlighted in green. B, dose-response curves for Cu(II)-bipyridine (i), Zn(II)-bipyridine (ii), and Cu(II)-phenanthrolene (iii) in respect of stimulation of IP3 turnover in COS-7 cells transiently transfected with the [GlyIII:05His; PheIII:08Ala]-CXCR3 construct (solid symbols). For comparison are shown the dose-response curves for the indicated metal ion chelator complex in the positive control [i.e., the [GlyIII:05His]-CXCR3 background construct (□) and in the negative control (i.e., the wild-type CXCR3 receptor) (△)]. C, dose-response curves for Cu(II)-bipyridine (i), Zn(II)-bipyridine (ii), and Cu(II)-phenanthrolene (iii) in respect of stimulation of IP3 turnover in COS-7 cells transiently transfected with the [GlyIII:05His; TyrVII:10Ala]-CXCR3 construct (solid symbols) with positive and negative controls as in B.

The present agonist tethering and activation mechanism is rather similar to that applied by Buck and Wells using covalent, disulfide tethering (Buck and Wells, 2005)—but with opposite orientation of the attachment site and the second-site interaction point (Fig. 8B). In an elegant study they made small thiol-reactive compounds act as agonists for the C5a receptor by tethering them to a Cys residue introduced at position VI:20 ($Gly^{262}Cys$). From this site, the compounds established second-site interactions with an Ile residue located at position III:08 (Ile^{116}) (i.e., one helical turn "below" the metal ion anchor-point, HisIII:05) (Buck and Wells, 2005). It is noteworthy that space-generating mutations at position III:08 increased potency and agonism for the CysVI:20 tethered ligands, whereas space-filling, steric hindrance mutagenesis at position III:08 decreased affinity and turned compounds into antagonists (Buck and Wells, 2005). These observations support the notion that agonism is associated with movement of the extracellular segments of TM-VI and TM-III toward each other.

As illustrated by the CXCR3 receptor in the present study, the opposing faces of the involved helices often provide much of the molecular equipment required for the stabilization of the active conformation—in this case, three of the four components of the "aromatic zipper." It is noteworthy, however, that the CXCR3 receptor does not display any sign of ligand independent or constitutive signaling efficacy. Thus, the in-

teraction of the three aromatic residues, PheIII:08, TyrVI:16, and TyrVII:10, is apparently not strong enough in the CXCR3 receptor to hold the receptor in its active conformation and thereby leads to ligand-independent signaling. However, in the ghrelin receptor, for example, a similar aromatic cluster on the opposing faces of TM-VI and VII—comprising PheVI:16, PheVII:06, and PheVII:09—is essential for the ~50% constitutive signaling activity of this receptor (Holst et al., 2004). Interestingly, naturally occurring mutations in the aromatic cluster (PheVI:16) selectively eliminate the constitutive activity of this receptor and lead to a clinical syndrome characterized by short stature and obesity (Holst and Schwartz, 2006; Pantel et al., 2006).

Large Molecule Agonists. Many agonists for 7TM receptors are large molecules, such as peptide hormones and chemokines, which are known to interact mainly with the N-terminal extension, the loop regions, and perhaps the extracellular ends of the helices (Schwartz and Holst, 2002; Schwarz and Wells, 2002; Vassart et al., 2004). It is interesting to note that the metal ion site-engineered CXCR3 receptor can be activated by both the large endogenous chemokine agonists and by the small metal ion chelator complexes. It is noteworthy that the three aromatic residues from TM-III, -VI, and -VII, which interdigitate to form the "aromatic zipper" deep in the pocket, are only essential for the agonist activity of the small molecule chelators and not at all for the large chemokine proteins (Table 2). In the past, we have found that a metal ion site-engineered NK1 receptor can be activated both by Zn(II) ions binding between positions III:08 and VII:06 and by the endogenous substance P neuropeptide acting at exterior epitopes (Holst et al., 1998, 2000). In that case, steric hindrance mutagenesis demonstrated that substance P does not reach deep down in the main ligand binding pocket to act as an agonist (Holst et al., 1998). It is proposed that large agonists such as chemokines, peptide hormones, and neuropeptides act as agonists by stabilizing a similar active conformation as presented in the present study for the small molecule aromatic chelators but that they do so by acting in a "Velcro-like" manner involving binding to multiple, more extracellular epitopes of the receptor. Such large agonists may or may not—in addition—interact with residues in the main ligand binding pocket. But that is not required. There does not seem to be a common "lock" for all the different agonist "keys" in 7TM receptor, but there is probably a common molecular activation mechanism (Schwartz and Rosenkilde, 1996). That is, the chemically highly diverse agonists are expected to stabilize similar active receptor conformations in their respective target receptors through binding in rather significantly different manners at different sites, depending on the size and chemical properties of the agonists (Elling et al., 2006).

Alternative Models for CXCR3 Receptor Activation. The results of the present study have above been discussed in relation to the global toggle switch model for 7TM receptor activation in which a large degree of induced fit is part of the ligand binding but where the activation mechanism is believed to be a result of a concerted action type of allostery (Elling et al., 2006; Schwartz et al., 2006). An alternative sequential type of allosteric model for 7TM activation has been advocated especially by Pardo and coworkers (Jongejan et al., 2005; Urizar et al., 2005). This model does not involve major conformational changes of the helical segments around

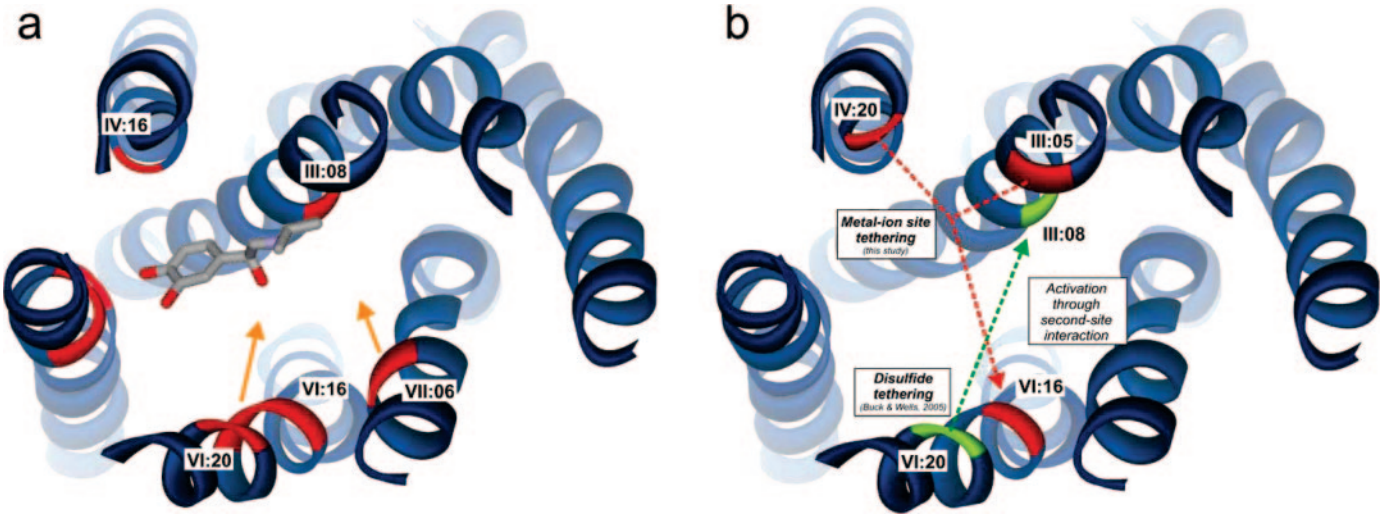

Fig. 8. Presumed binding site residues and activation mechanism for two tethered small-molecule agonists compared with a prototype agonist in 7TM receptors. A, interaction residues in the β_2-adrenergic receptor for the freely diffusible agonist isoproterenol. In a molecular model of the backbone of the seven helical bundle from the X-ray structure of the dark, inactive state of rhodopsin—shown in solid ribbon format—the position of the presumed agonist binding residues are indicated in red. A stick model of isoproterenol illustrate the spatial gap to the interaction residues in especially TM-VI in accordance with the prevailing induced fit binding models (Carmine et al., 2004; Kobilka, 2004; Liapakis et al., 2004; Swaminath et al., 2004). Orange arrows indicate the presumed inward movements of the extracellular segments of TM-VI and -VII according to the global toggle switch activation model (Elling et al., 2006). B, binding sites for tethered ligands—comparison of the metal ion site-tethering approach of the present study with the disulfide-tethering approach of Buck and Wells (2005). Positions IV:20 and III:05, which are used for the metal ion site tethering of the aromatic chelators as well as position VI:16 identified as the main second-site interaction point, are all indicated in red (data from the present study). In green are highlighted position VI:20 used for covalent disulfide tethering of small thiol-reactive compounds, which act as agonists by making second-site interactions with an Ile in position III:08 (also shown in green) (Buck and Wells, 2005). Introduction of a space-filling Trp residue at position III:08 decreased affinity and turned compounds into antagonists, whereas Ala in position III:08 increased affinity and turned compounds into agonists. Thus in both of these cases of relatively well defined, "anchored" ligands as well as in the monoamine case (A), the small molecule agonist binds between TM-III, -V, -VI, and -VII and apparently acts through holding the extracellular segments of TM-VI and -VII in an inwardly bent conformation in agreement with the Global Toggle Switch activation mechanism (Schwartz et al., 2006).

the main ligand binding crevice; instead, it requires that the agonist touch key residues, which, through a "domino effect" from residue to residue down through the helical bundle, eventually release the major conformational changes occurring at the intracellular face of the receptor. Key residues in this model are residues III:12 (3.36), VII:12 (7.45), VI:13 (6.48); VII:16 (7.49), II:10 (2.50), and III:26 (3.50) (Jongejan et al., 2005; Urizar et al., 2005). We agree that these and other more-or-less conserved residues will change, for example, rotamer states and/or hydrogen bond partners during receptor activation. But we consider these conformational changes to be part of the concerted global toggle switch mechanism. Nevertheless, in the case of the bipyridine agonist, it could in principle act solely by touching PheIII:12, which is located at the bottom of the proposed binding pocket—corresponding to SerIII:12 in the histidine H1 receptor (Jongejan et al., 2005). However, it should be noted that when PheIII:12 was mutated as part of the search for second-site interactions in the CXCR3 receptor, very little effect was observed on the agonism of, for example, bipyridine (Table 2). However, the present study was not designed to try to differentiate between the two models for receptor activation. Recently a novel X-ray structure of a presumed active form of rhodopsin was presented in which minimal changes of the helical bundle had occurred (Salom et al., 2006). This does not fit with either of the above discussed models, which both incorporate major conformational changes of at least the intracellular helical segments (Hubbell et al., 2003).

Design and Development of Nonpeptide Agonists for 7TM Receptors. In relation to drug discovery, the observation that it is possible to make a small, simple ligand such as bipyridine act as an efficient agonist—even a superagonist—for a receptor, which normally is activated by a large chemokine protein is notable. Especially because this is achieved simply by ensuring that the small ligand through a single point mutation is tethered at the right position in the main ligand-binding pocket. This indicates that it should be possible to design and develop small molecule agonists for 7TM receptors in general (i.e., based on knowledge of the physicochemical properties of the binding pocket); importantly, the binding pocket presented in the *active* receptor conformation.

Acknowledgments

We thank Lisbet Elbak and Inger Smith Simonsen for excellent technical help throughout this study.

References

Ballesteros JA, Jensen AD, Liapakis G, Rasmussen SG, Shi L, Gether U, and Javitch JA (2001) Activation of the β_2-adrenergic receptor involves disruption of an ionic lock between the cytoplasmic ends of transmembrane segments 3 and 6. *J Biol Chem* **276:**29171–29177.

Berridge MJ, Dawson MC, Downes CP, Heslop JP, and Irvin RF (1983) Changes in the level of inositol phosphates after agonist-dependent hydrolysis of membrane phosphoinositides. *Biochem J* **212:**473–482.

Bockaert J and Pin JP (1999) Molecular tinkering of G protein-coupled receptors: an evolutionary success. *EMBO (Eur Mol Biol Organ) J* **18:**1723–1729.

Buck E and Wells JA (2005) Disulfide trapping to localize small-molecule agonists and antagonists for a G protein-coupled receptor. *Proc Natl Acad Sci USA* **102:** 2719–2724.

Carmine RD, Molinari P, Sbraccia M, Ambrosio C, and Costa T (2004) "Induced-fit" mechanism for catecholamine binding to the β_2-adrenergic receptor. *Mol Pharmacol* **66:**356–363.

Elling CE, Frimurer TM, Gerlach LO, Jorgensen R, Holst B, and Schwartz TW (2006) Metal-ion site engineering indicating a global toggle switch model for 7TM receptor activation. *J Biol Chem* **281:**17337–17343.

Farrens DL, Altenbach C, Yang K, Hubbell WL, and Khorana HG (1996) Requirement of rigid-body motion of transmembrane helices for light activation of rhodopsin. *Science (Wash DC)* **274:**768–770.

Gerlach LO, Jakobsen JS, Jensen KP, Rosenkilde MR, Skerlj RT, Ryde U, Bridger GJ, and Schwartz TW (2003) metal ion enhanced binding of AMD3100 to Asp262 in the CXCR4 receptor. *Biochemistry* **42:**710–717.

Gether U, Lin S, Ghanouni P, Ballesteros JA, Weinstein H, and Kobilka BK (1997) Agonist induced conformational changes in transmembrane domains III and VI of the beta2 adrenoceptor. *EMBO (Eur Mol Biol Organ) J* **16:**6737–6747.

Han SJ, Hamdan FF, Kim SK, Jacobson KA, Bloodworth LM, Li B, and Wess J (2005) Identification of an agonist-induced conformational change occurring adjacent to the ligand-binding pocket of the m_3 muscarinic acetylcholine receptor. *J Biol Chem* **280:**34849–34858.

Hendlich M, Bergner A, Gunther J, and Klebe G (2003) Relibase: design and development of a database for comprehensive analysis of protein-ligand interactions. *J Mol Biol* **326:**607–620.

Holst B, Elling CE, and Schwartz TW (2000) Partial agonism through a zinc-ion switch constructed between transmembrane domains III and VII in the tachykinin NK_1 Receptor. *Mol Pharmacol* **58:**263–270.

Holst B, Holliday ND, Bach A, Elling CE, Cox HM, and Schwartz TW (2004) Common structural basis for constitutive activity of the ghrelin receptor family. *J Biol Chem* **279:**53806–53817.

Holst B and Schwartz TW (2006) Ghrelin receptor mutations–too little height and too much hunger. *J Clin Investig* **116:**637–641.

Holst B, Zoffmann S, Elling CE, Hjorth SA, and Schwartz TW (1998) Steric hindrance mutagenesis versus alanine scan in mapping of ligand binding sites in the tachykinin NK1 receptor. *Mol Pharmacol* **53:**166–175.

Hubbell WL, Altenbach C, Hubbell CM, and Khorana HG (2003) Rhodopsin structure, dynamics, and activation: a perspective from crystallography, site-directed spin labeling, sulfhydryl reactivity, and disulfide cross-linking. *Adv Protein Chem* **63:**243–290.

Jongejan A, Bruysters M, Ballesteros JA, Haaksma E, Bakker RA, Pardo L, and Leurs R (2005) Linking agonist binding to histamine H1 receptor activation. *Nat Chem Biol* **1:**98–103.

Kobilka B (2004) Agonist binding: a multistep process. *Mol Pharmacol* **65:**1060–1062.

Kostenis E, Zeng FY, and Wess J (1998) Functional characterization of a series of mutant G protein α_q subunits displaying promiscuous receptor coupling properties. *J Biol Chem* **273:**17886–17892.

Lefkowitz RJ (2004) Historical review: a brief history and personal retrospective of seven-transmembrane receptors. *Trends Pharmacol Sci* **25:**413–422.

Li J, Edwards PC, Burghammer M, Villa C, and Schertler GF (2004) Structure of bovine rhodopsin in a trigonal crystal form. *J Mol Biol* **343:**1409–1438.

Li Z and Scheraga HA (1987) Monte Carlo-minimization approach to the multiple-minima problem in protein folding. *Proc Natl Acad Sci USA* **84:**6611–6615.

Liapakis G, Chan WC, Papadokostaki M, and Javitch JA (2004) Synergistic contributions of the functional groups of epinephrine to its affinity and efficacy at the β_2 adrenergic receptor. *Mol Pharmacol* **65:**1181–1190.

Okada T, Sugihara M, Bondar AN, Elstner M, Entel P, and Buss V (2004) The retinal conformation and its environment in rhodopsin in light of a new 2.2 Å crystal structure. *J Mol Biol* **342:**571–583.

Palczewski K, Kumasaka T, Hori T, Behnke CA, Motoshima H, Fox BA, Le Trong I, Teller DC, Okada T, Stenkamp RE, et al. (2000) Crystal structure of rhodopsin: a G protein-coupled receptor. *Science (Wash DC)* **289:**739–745.

Pantel J, Legendre M, Cabrol S, Hilal l, Hajaji Y, Morisset S, Nivot S, Vie-Luton MP, Grouselle D, de Kerdanet M, et al. (2006) Loss of constitutive activity of the growth hormone secretagogue receptor in familial short stature. *J Clin Investig* **116:**760–768.

Rosenkilde MM, Gerlach LO, Jakobsen JS, Skerlj RT, Bridger GJ, and Schwartz TW (2004) Molecular mechanism of AMD3100 antagonism in the CXCR4 receptor: transfer of binding site to the CXCR3 receptor. *J Biol Chem* **279:**3033–3041.

Rosenkilde MM, Kledal TN, Brauner-Osborne H, and Schwartz TW (1999) Agonists and inverse agonists for the herpesvirus 8-encoded constitutively active seven-transmembrane oncogene product, ORF-74. *J Biol Chem* **274:**956–961.

Ruprecht JJ, Mielke T, Vogel R, Villa C, and Schertler GF (2004) Electron crystallography reveals the structure of metarhodopsin I. *EMBO (Eur Mol Biol Organ) J* **23:**3609–3620.

Sakmar TP, Menon ST, Marin EP, and Awad ES (2002) Rhodopsin: insights from recent structural studies. *Annu Rev Biophys Biomol Struct* **31:**443–484.

Salom D, Lodowski DT, Stenkamp RE, Trong IL, Golczak M, Jastrzebska B, Harris T, Ballesteros JA, and Palczewski K (2006) Crystal structure of a photoactivated deprotonated intermediate of rhodopsin. *Proc Natl Acad Sci USA* **103:**16123–16128.

Schwartz TW, Frimurer TM, Holst B, Rosenkilde MM, and Elling CE (2006) Molecular mechanism of 7TM receptor activation—a global toggle switch model. *Annu Rev Pharmacol Toxicol* **46:**481–519.

Schwartz TW, Gether U, Schambye HT, and Hjorth SA (1995) Molecular mechanism of action of non-peptide ligands for peptide receptors. *Curr Pharmaceut Design* **1:**325–342.

Schwartz TW and Holst B (2006) Ago-allosteric modulation and other types of allostery in 7TM receptors. *J Recept Signal Transduct* **26:**107–128.

Schwartz TW and Holst B (2002) Molecular structure and function of 7TM/G-protein coupled receptors, in *Textbook of Receptor Pharmacology* (Forman JC and Johansen T eds) pp 65–84, CRC Press, Bocan Rouge, FL.

Schwartz TW and Rosenkilde MM (1996) Is there a 'lock' for all 'keys' in 7TM receptors. *Trends Pharmacol Sci* **17:**213–216.

Schwarz MK and Wells TN (2002) New therapeutics that modulate chemokine networks. *Nat Rev Drug Discov* **1:**347–358.

Shi L and Javitch JA (2002) The binding site of aminergic G protein-coupled receptors: the transmembrane segments and second extracellular loop. *Annu Rev Pharmacol Toxicol* **42:**437–467.

Strader CD, Gaffney T, Sugg EE, Candelore MR, Keys R, Patchett AA, and Dixon RAF (1991) Allele-specific activation of genetically engineered receptors. *J Biol Chem* **266:**5–8.

Swaminath G, Xiang Y, Lee TW, Steenhuis J, Parnot C, and Kobilka BK (2004) Sequential binding of agonists to the β_2 adrenoceptor. Kinetic evidence for intermediate conformational states. *J Biol Chem* **279:**686–691.
Urizar E, Claeysen S, Deupi X, Govaerts C, Costagliola S, Vassart G, and Pardo L (2005) An activation switch in the rhodopsin family of G protein-coupled receptors: the thyrotropin receptor. *J Biol Chem* **280:**17135–17141.
Vassart G, Pardo L, and Costagliola S (2004) A molecular dissection of the glycoprotein hormone receptors. *Trends Biochem Sci* **29:**119–126.
Wieland K, Zuurmond HM, Krasel C, IJzerman AP, and Lohse MJ (1996) Involvement of Asn-293 in stereospecific agonist recognition and in activation of the beta2-adrenergic receptor. *Proc Natl Acad Sci USA* **93:**9276–9281.

Address correspondence to: Thue W. Schwartz, Laboratory for Molecular Pharmacology, Department of Pharmacology, The Panum Institute, University of Copenhagen, Blegdamsvej 3b, DK-2200, Copenhagen, Denmark. E-mail: schwartz@molpharm.dk